



**HAL**  
open science

## **Analysis of Boundary-Layer Statistical Properties at Dome C, Antarctica**

Jean-François Rysman, Sébastien Verrier, Alain Lahellec, Christophe Genthon

► **To cite this version:**

Jean-François Rysman, Sébastien Verrier, Alain Lahellec, Christophe Genthon. Analysis of Boundary-Layer Statistical Properties at Dome C, Antarctica. *Boundary-Layer Meteorology*, 2015, 156 (1), pp.145-155. <10.1007/s10546-015-0024-x>. <insu-01143166>

**HAL Id: insu-01143166**

**<https://insu.hal.science/insu-01143166v1>**

Submitted on 14 Sep 2015

**HAL** is a multi-disciplinary open access archive for the deposit and dissemination of scientific research documents, whether they are published or not. The documents may come from teaching and research institutions in France or abroad, or from public or private research centers.

L'archive ouverte pluridisciplinaire **HAL**, est destinée au dépôt et à la diffusion de documents scientifiques de niveau recherche, publiés ou non, émanant des établissements d'enseignement et de recherche français ou étrangers, des laboratoires publics ou privés.



HAL Authorization

1 **Analysis of Boundary Layer Statistical Properties at**  
2 **Dome C, Antarctica**

3 **Jean-François Rysman · Sébastien**  
4 **Verrier · Alain Lahellec · Christophe**  
5 **Genthon**

6 **Abstract** The boundary layer of the Antarctic Plateau is unique on account  
7 of its isolated location and extreme stability. This study investigates the char-  
8 acteristics of this boundary layer using wind and temperature measurements  
9 from a 45-m high tower located at Dome C. First, spectral analysis reveals  
10 that both fields have a scaling behaviour from 30 minutes to 10 days (spectral  
11 slope  $\beta \approx 2$ ). Wind and temperature time series also shows a multifractal  
12 behaviour. Therefore, it is possible to fit the moment-scaling function to the  
13 universal multifractal model and obtain multifractal parameters for temper-  
14 ature ( $\alpha \approx 1.51$  and  $C_1 \approx 0.14$ ) and wind speed ( $\alpha \approx 1.34$  and  $C_1 \approx 0.13$ ).  
15 The same analysis is repeated separately in winter and summer at six different  
16 heights. The  $\beta$  parameter shows a strong stratification with height especially in

---

JF Rysman  
UPMC Univ. Paris 06; Université Versailles St-Quentin; CNRS/INSU, LATMOS-IPSL,  
France E-mail: jfrysman@lmd.polytechnique.fr

S Verrier  
LOCEAN (UPMC/IPSL), CNES, France

A Lahellec  
Laboratoire de Météorologie Dynamique, UPMC Univ. Paris 06, France

C Genthon  
UJF - Grenoble 1 / CNRS Laboratoire de Glaciologie et Géophysique de l'Environnement  
(LGGE), France

17 summer. This means that properties of turbulence change surprisingly rapidly  
18 from the ground to the top of the tower.

19 **Keywords** Boundary Layer · Dome C · Meteorological tower · Scaling ·  
20 Statistical properties

## 21 **1 Introduction**

22 The Antarctic surface consists of a plateau ranging from 2000 to 4000 m in  
23 altitude and covered 98 % by ice (King and Turner, 1997). One of its local  
24 maxima is Dome C (3233 m), where the Concordia station has been installed  
25 since 1997. At this station, meteorological measurements are taken at the sur-  
26 face with an automated weather station, while daily launched balloons pro-  
27 vide soundings of the troposphere. As snow surface emissivity is higher than  
28 atmosphere emissivity, significant temperature inversion exists in this region  
29 at night and during winter (Hudson and Brandt, 2005; Genthon et al., 2013).  
30 Moreover, surface winds are weak over the Eastern Antarctic Plateau where  
31 the surface is smooth. These features, which inhibit turbulence and vertical  
32 motions, explain the extremely stable boundary layer at Dome C. The bound-  
33 ary layer may remain stable for several months almost without interruption,  
34 leading to remarkable properties. The analysis of these properties is of high in-  
35 terest to meteorologists since it provides the opportunity to better understand  
36 the characteristics of an extremely stable boundary layer in an unperturbed  
37 environment and facilitates the development of parameterizations aimed at  
38 global and regional models.

39 Overall, boundary layer properties in Antarctica are poorly studied com-  
40 pared with mid-latitude boundary layer properties because of the difficulty in  
41 performing surface measurements. To fill this gap, a tower was installed in  
42 2007 close to the Concordia station. Instruments were set up to measure wind,

43 temperature, and humidity at six levels along the 45 m tower. At present, this  
44 is the highest tower that performs continuous measurements in Antarctica.  
45 As the boundary layer depth in Antarctica is very shallow, the vertical vari-  
46 ability is considerable and, for this reason, a tower is well adapted to study  
47 boundary layer characteristics. The continuous measurements along the ver-  
48 tical are particularly interesting when studying the boundary layer temporal  
49 evolution and especially when analyzing the transition between the stable and  
50 convective boundary layer that occurs on summer days.

51 In most Antarctic stations, except for the South Pole and Halley stations,  
52 in-situ measurements are simply taken at standard meteorological levels (2  
53 and 10 m). In addition, some measurement campaigns at high latitude regions  
54 have been performed with an instrumented mast (e.g., King and Turner, 1997;  
55 Travouillon et al., 2003; Grachev et al., 2005). As a result, long-term, in-situ,  
56 and high-quality measurements of the low atmosphere at high latitude are  
57 scarce and extremely valuable.

58 The present study is based on wind and temperature observations collected  
59 from the tower at Dome C between January and December 2009. The objective  
60 was to study the statistical properties of wind and temperature of the Dome C  
61 boundary layer together with the vertical variability of these properties. The  
62 analysis of the boundary layer is often difficult since processes with various  
63 spatial and temporal scales occur conjointly. However, statistical properties  
64 known as scaling or self-similarity can characterize this complex system with  
65 only a few parameters. Experimental measurements have shown that scaling  
66 properties are found in most geophysical fields and are related to atmospheric  
67 turbulence, notably wind and temperature (Gage and Nastrom, 1986), cloud  
68 radiance (Tessier et al., 1993), and rainfall (Verrier et al., 2011; Rysman et al.,  
69 2013)). As a result, we chose to use this approach in this paper.

70 First, we highlight and analyze the scaling behaviour of wind and tem-  
71 perature fields. In the second part of this analysis, we use the multifractal  
72 framework to obtain parameters that describe the fields intrinsic properties.  
73 This is the first time that such an innovative analysis is conducted in Antarc-  
74 tica and for such an extremely stable boundary layer. This approach allows us  
75 to characterize the full spectrum of signal variability that is not possible with  
76 standard approaches.

## 77 **2 Data**

78 The Concordia scientific station is based on a local maxima called Dome C  
79 ( $75^{\circ} 06' S$ ,  $123^{\circ} 20' E$ , 3233 m a.s.l.) in the eastern part of the Antarctic  
80 Plateau. The nearest coast is located more than 1000 km away. The local  
81 slope of the Dome is about  $5 \times 10^{-4}$  toward the north and  $1 \times 10^{-3}$  toward the  
82 east (based on NASA measurements at a 10' resolution). At this latitude, the  
83 sun culminates at  $38^{\circ}$  on 21 December, and the winter night extends between  
84 April and September.

85 In this study, we used meteorological instruments deployed along a 45 m  
86 tower located 700 m from the Concordia station. The tower position was chosen  
87 with respect to the atmospheric flow in order to minimize the influence of  
88 station buildings. Six Vaisälä hygrometers (4 HMP155 and 2 HMP45AC),  
89 six pt100 DIN IEC 751 thermistors, and six Young 45106 aero-vanes were  
90 mounted at 3.6 m, 11 m, 18.6 m, 25.9 m, 33.2 m, and 42.4 m. Measurements  
91 were performed with a 10-second time step and averaged over 30 minutes.  
92 Additional technical details can be found in Genthon et al. (2010, 2013).

### 93 **3 Methodology**

#### 94 **3.1 Scaling**

95 Initially, approaches based on a single exponent, called monofractal approaches,  
 96 were used to characterize the scaling properties of a field over a given inertial  
 97 range. Among these approaches, spectral analysis is widely used. It has been  
 98 shown that if a physical field presents scaling properties, its power spectral  
 99 density  $E$  (Priestley , 1981), proportional to the square of the modulus of the  
 100 Fourier transform of the field, follows power-law behaviour as a function of  
 101 frequency  $f$  (i.e., log-log linearity):

$$102 \quad E(f) \simeq f^{-\beta} \quad (1)$$

103 The  $\beta$  value depends on the correlation in a given field: a highly correlated  
 104 field has a high  $\beta$  exponent, while a white noise (uncorrelated field) has a  $\beta$   
 105 exponent equal to zero (for details, see Rysman et al. (2013)).

106 Another way to highlight the scaling behaviour of a field is to test the first-  
 107 order structure function log-log linearity. The first-order structure function  
 108 corresponds to the statistical average of the absolute increments for different  
 109 lags (this is a first-order function analogue to variograms):

$$110 \quad S(\delta t) = \langle |X(t + \delta t) - X(t)| \rangle \simeq \delta t^H \quad (2)$$

111 where  $\delta t$  is the time lag (varying from 0 to the time series length),  $S$  the first-  
 112 order structure function and  $\langle \rangle$  is the ensemble averaging operator. As for  $\beta$ ,  
 113  $H$  indicates the smoothness of the field.

### 114 3.2 Multifractal

115 Subsequently, refinements were proposed in order to take into account the  
 116 strong inhomogeneity in the energy fluxes (e.g., Yaglom, 1966). These refine-  
 117 ments rely on multiplicative cascades, that is, the representation of multiscale  
 118 variability using a sequence of iterative multiplicative modulations of increas-  
 119 ing resolution (e.g., Schertzer and Lovejoy, 1987; She and Leveque, 1994).  
 120 Such models can usually be parameterized using a few exponents with more  
 121 or less obvious physical interpretations, thus giving a description of a much  
 122 wider class of variability than monofractal models (single parameter models).  
 123 More precisely, multiplicative cascades generate multifractal stochastic fields.  
 124 To investigate the validity of these theories with geophysical data, multifractal  
 125 analysis procedures are applied (e.g., Verrier et al., 2011). The latter relies on  
 126 the remarkable scaling properties of statistical moments of different orders that  
 127 generalize the spectral scaling properties to a wider class of process intensities.

128 Statistically speaking, a field  $\Phi$  follows multifractal properties if the statis-  
 129 tical moments of the field depend on the resolution in a power-law manner. The  
 130 power-law exponent only depends on the moment order, so that the statistical  
 131 moments of the normalized field can be expressed as:

$$132 \quad \langle \Phi_\lambda^q \rangle \simeq \lambda^{K(q)} \quad (3)$$

133 where  $\langle \rangle$  is the ensemble averaging operator,  $q$  the moment order (non-  
 134 necessarily integer),  $\lambda$  the resolution, and  $K(q)$  the moment-scaling function,  
 135 which relates to scaling exponents and moments. In the following, the empirical  
 136 statistical moments are denoted as  $M_q(\lambda)$ .

137 Several parameterizations of the fundamental moment-scaling function  $K(q)$   
 138 exist (e.g., Schertzer and Lovejoy, 1987; She and Leveque, 1994). In this pa-  
 139 per, we consider the two-parameter universal form defined by Schertzer and

140 Lovejoy (1987).  $K(q)$  is thus parametrized by two fundamental parameters,  
 141  $C_1$  (intermittency parameter) and  $\alpha$  (index of multifractality):

$$142 \quad K(q) = \frac{C_1}{\alpha - 1}(q^\alpha - q) \quad (4)$$

143 where  $\alpha \in [0 : 2]$  and  $\alpha \neq 1$  and  $C_1 \in [0 : D]$  with  $D$  the dimension of the  
 144 Euclidean space in which the field is defined (i.e., 1 in the case of time series).

145 A physical understanding of these parameters allows a given geophysical  
 146 field to be characterized.  $C_1$  can be related to the intermittency of the data,  
 147 that is, the uniformity of the data around the mean. It increases as most of the  
 148 measured values depart from the mean.  $\alpha$  relates to the presence of extreme  
 149 fluctuations within the field. High values of  $\alpha$  indicate a field with a few large  
 150 singularities (for details on the interpretation of multifractal parameters, see  
 151 Pecknold et al., 1993; Purdy et al., 2001; Nykanen, 2008).

152 Often,  $\Phi$  cannot be directly related to geophysical fields, because most of  
 153 these fields and atmospheric processes are better described as low-pass filtered  
 154 versions of multiplicative cascades. Therefore, a scaling filter such as fractional  
 155 integration is usually applied (Schertzer and Lovejoy, 1987). Consequently,  
 156 the properties of the conservative multifractal field  $\Phi$  should be distinguished  
 157 from the (usually) non-conservative integrated fields (the term integrated is  
 158 related to the fractional integration needed to transform a conservative (non  
 159 integrated) multifractal field to a realistic physical field (non conservative and  
 160 integrated)).

161 The first step of a multifractal analysis is to determine whether the studied  
 162 field is integrated. To this end, we use spectral analysis: if a field is integrated,  
 163 its spectral slope is strictly (and notably) greater than 1. We then use the  
 164 structure function. Indeed, the  $H$  exponent gives the order of fractional inte-  
 165 gration in the field and physically represents the degree of smoothing involved

166 with the integration. For instance,  $H = 0$  is associated with a conservative  
 167 cascade (for details, see de Montera et al., 2009).

## 168 4 Results

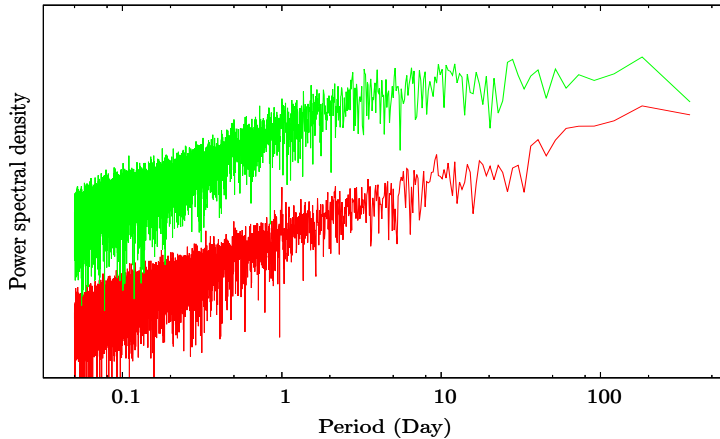


**Fig. 1** Power spectral density of temperature ( $\text{K}^2 \text{s}^{-1}$ , red line) and zonal wind ( $\text{m}^2 \text{s}^{-3}$ , green line) at 42.4 m in a log-log plot

169 Figure 1 reveals that the power spectral density of zonal wind and temper-  
 170 ature scale with a slope of respectively 2.20 and 2.02 at 42.4 m (from 2 hours  
 171 up to 10 days). In other words, a high temporal autocorrelation exists be-  
 172 tween these fields, with the temperature at a given time being related to the  
 173 temperature up to 10 days later. For longer periods of time, both fields ap-  
 174 pear uncorrelated (spectral slope equals zero) because the meteorological noise  
 175 is greater than the remaining correlation. The region with periods exceeding  
 176 10 days is often called the spectral plateau. The spectral plateau has been  
 177 highlighted in various meteorological fields in the past (Fraedrich and Larn-  
 178 der, 1993; Olsson, 1995; Fabry, 1996; Lovejoy and Schertzer, 2011; Rysman  
 179 et al., 2013), with a decorrelation period ranging from 5 days to 1 month,  
 180 which reveals a similarity among meteorological fields independent of local

181 characteristics. It must also be emphasized that both spectra are very similar  
182 (similar slope and scaling range), suggesting a relationship between both vari-  
183 ables. This similarity can be related to the influence of wind on temperature;  
184 for example, when the wind changes direction, local temperature is affected.

185 Since spectral slopes greater than 1 are notably observed, it means that  
186 the fields are integrated. The next step is to determine the degree of fractional  
187 integration in the fields. Figure 2 shows the first-order structure functions of  
188 the temperature and zonal wind series, averaged over height. Regarding tem-  
189 perature, data only pertains to the period from January to October because  
190 temperature sensors were interrupted for a few hours in October. For both  
191 temperature and zonal wind, a scaling behaviour is found between 2 and 16 h  
192 with an exponent  $H$  of about 0.69 (temperature) and 0.66 (zonal wind). This  
193 confirms that for both variables, the observables should perhaps be related to  
194 multifractal field only when applying a fractional integration. This is achieved  
195 following Lavallée et al. (1993) and de Montera et al. (2009) with the compu-  
196 tation of the absolute gradient of the time series.

197 The empirical moments of the latter are then estimated in order to confirm  
198 the validity of Eq. 3. In a log-log plot, the multiscaling behaviour of moments  
199 appears as a sequence of straight lines, each associated with a unique moment  
200 order. Figure 3 shows the behaviour of statistical moments (between 0 and 2)  
201 of temperature and zonal wind as a function of scale in log-log coordinates.  
202 Two regimes thus appear: from 2 h to 2 days and from 2 days to 0.5 month. Red  
203 lines at high frequencies show the fit of moment laws in the range 2 h-2 days.  
204 In this range of scales, the moments (especially high-order moments) strongly  
205 vary with the scale in a way that might be approximated by multifractal  
206 laws. Larger scales are characterized by much slighter variations of moments,  
207 represented by flat curves at low frequencies. This confirms the findings of  
208 the structure function analysis above, wherein a scaling regime was found at

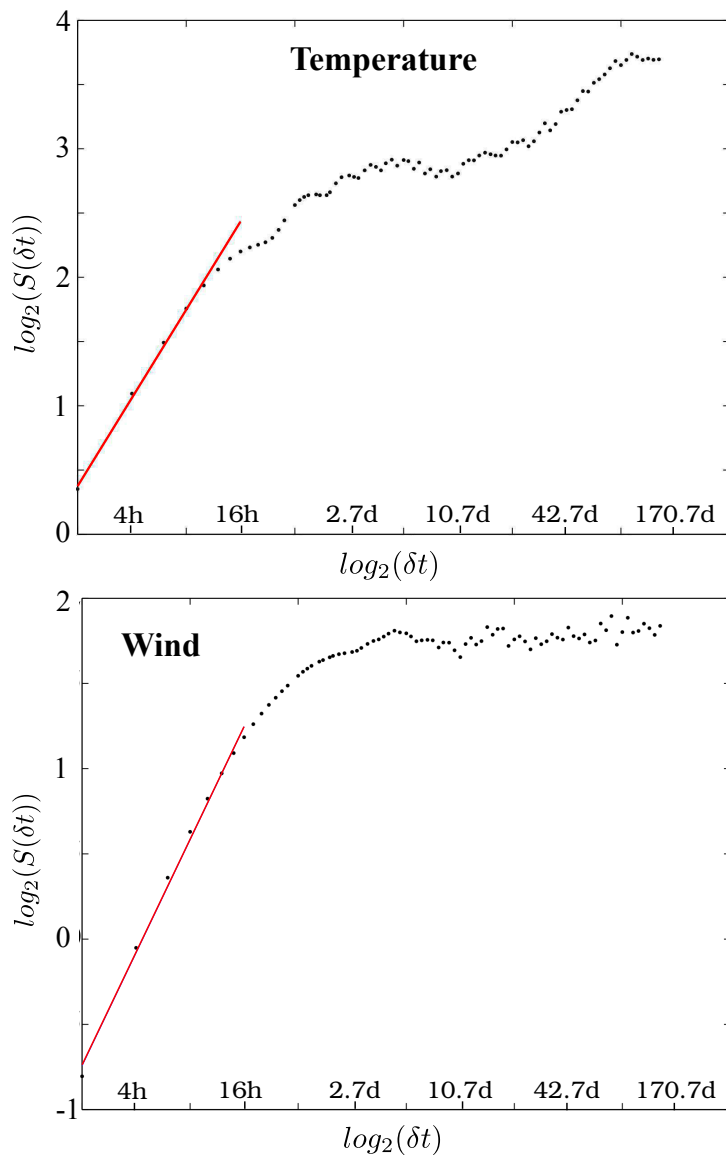


**Fig. 2** First-order structure function ( $S(\delta t)$ ) of temperature (K) and zonal wind (m.s<sup>-1</sup>) averaged over heights as a function of time lag ( $\delta t$ ) ranging from 2 h to 170.7 days. Linear regressions between 2 and 16 h are shown as red lines

209 high frequencies, while all statistics had more regular scale behaviour on larger  
 210 scales.

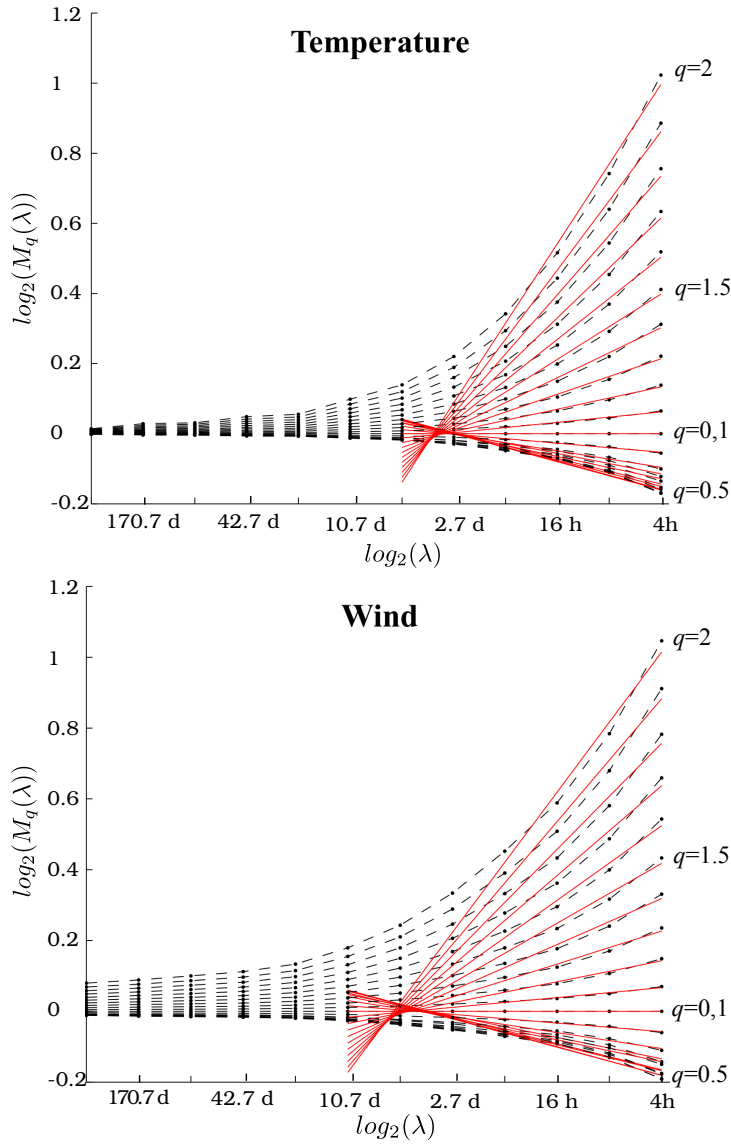


**Fig. 3** Empirical moments ( $M_q(\lambda)$ ) of the absolute temperature and zonal wind temporal gradients, averaged over heights as a function of the resolution ranging from 2 h to 170.7 days (log-log plot). Each straight line corresponds to a linear regression of the moments of fixed order  $q$ . The orders taken into consideration are  $q = 0, 0.1, 0.2, \dots, 2.0$

211 Previous figures showed that zonal wind and temperature fields have mul-  
 212 tifractal behaviour. The next step focusses on the multifractal parametrization  
 213 of the 2 h-2 days regime in order to obtain  $C_1$  and  $\alpha$  parameters. Here, the

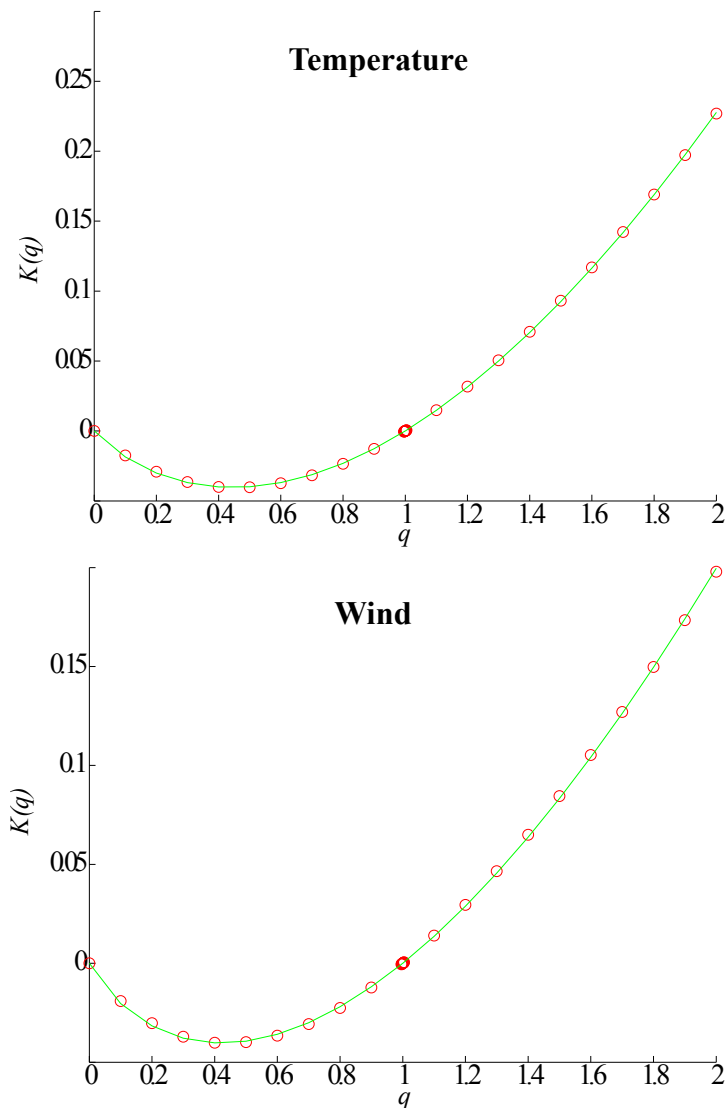


**Fig. 4** Empirical moment-scaling function ( $K(q)$ ) (red points), i.e., log-log slopes of the red fit lines in figure 3 and fit with universal multifractal model (green line) between 2 hours and 2 days for temperature and zonal wind averaged over height

214 slopes of the red fit lines previously computed are represented as a function  
 215  $K(q)$  for moment order  $q$  (Figure 4). The curve of the empirical scaling ex-  
 216 ponents  $K(q)$  is superimposed to the least-square best fit of the universal ( $\alpha$ ,  
 217  $C_1$ ) form. First, we observe that the fits are very accurate, thus validating

218 the choice of parameterization proposed by Schertzer and Lovejoy (1987). The  
219 best-fit parameters are  $\alpha \approx 1.51$  and  $C_1 \approx 0.14$  for temperature and  $\alpha \approx 1.34$   
220 and  $C_1 \approx 0.13$  for zonal wind.

221 These parameters are consistent with previous multifractal analyses. For  
222 instance, Schmitt et al. (1992) using laboratory observations obtained  $\alpha \approx 1.2$   
223 and  $C_1 \approx 0.15$  for temperature and  $\alpha \approx 1.3$  and  $C_1 \approx 0.25$  for wind. Further,  
224 Stolle et al. (2009); Lovejoy and Schertzer (2010); Stolle et al. (2012) using  
225 model outputs from tropical and mid-latitude regions obtained, in average, for  
226 wind and temperature  $\alpha \approx 1.8$  and  $C_1 \approx 0.12$ . The most significant difference  
227 is found for the  $\alpha$  parameter, which is lower in our observations compared to  
228 the model outputs in tropical and mid-latitude regions. This could indicate  
229 that our observations have less extreme values. However, it is difficult to give  
230 further interpretation because of the substantial differences between datasets.  
231 Additional analysis and measurements are thus required in order to deter-  
232 mine whether temperature and wind statistical properties significantly differ  
233 at Dome C compared to other parts of the world.

234 Overall, the monofractal and multifractal results reveal the intrinsic quality  
235 of the data. Indeed, positive slopes for spectra and moments highlight the  
236 organisation (or correlation) within the geophysical field (see Nykanen, 2008;  
237 Rysman et al., 2013), meaning that the noise of data is low compared to the  
238 meteorological signal. Moreover, most of the fits show a rather low noise.

239 Turning to the effect of elevation and season on scaling parameters, the  
240 same scaling analysis was applied separately to continuous period of summer  
241 (January-February) and winter (July-August) seasons for each height (table  
242 1).

243 Table 1 shows that scaling parameters depend on the season and height.  
244 Overall parameters are lower during winter (e.g., for wind  $\beta \simeq 2.00 \pm 0.03$ )  
245 than during summer (e.g., for wind  $\beta \simeq 2.21 \pm 0.09$ ). Moreover, during winter,

**Table 1** Multifractal parameters as a function of height and season (Summer (January-February) and Winter (July-August)). Missing data are indicated by a - and correspond to periods of interruptions for temperature sensors

Height (m)	Winter			
	Wind		Temperature	
	$\beta$	$H$	$\beta$	$H$
3.6	2.01±0.18	0.68±0.09	2.25±0.17	0.74±0.10
11	1.95±0.21	0.65±0.10	2.11±0.20	0.72±0.06
18.4	1.97±0.22	0.68±0.13	-	-
25.9	2.05±0.17	0.67±0.11	-	-
33.2	2.00±0.14	0.65±0.10	1.95±0.24	0.66±0.09
42.4	2.00±0.23	0.64±0.11	2.00±0.22	0.69±0.09
Summer				
3.6	2.06±0.17	0.68±0.05	2.14±0.22	0.91±0.03
11	2.14±0.14	0.72±0.04	2.05±0.23	0.85±0.06
18.4	2.22±0.13	0.75±0.04	1.89±0.28	0.75±0.07
25.9	2.26±0.12	0.74±0.04	1.91±0.17	0.71±0.06
33.2	2.28±0.14	0.75±0.04	1.92±0.18	0.69±0.05
42.4	2.29±0.13	0.75±0.04	1.89±0.23	0.68±0.06

<sup>246</sup>  $\beta$  (2.00±0.03) and  $H$  (0.66±0.02) are rather constant with height for zonal  
<sup>247</sup> wind while  $\beta$  and  $H$  decrease from the ground to the top of the tower for tem-  
<sup>248</sup> perature (from 2.25 to 2 for  $\beta$  and from 0.74 to 0.69 for  $H$ ). During summer,  
<sup>249</sup> the zonal wind shows a stratification with height for the  $H$  (from 0.68 to 0.75)  
<sup>250</sup> and the  $\beta$  parameters (2.06 to 2.29). Regarding temperature,  $H$  parameter  
<sup>251</sup> goes from 0.91 to 0.68 and  $\beta$  goes from 2.14 to 1.89. The  $C_1$  and  $\alpha$  parameters  
<sup>252</sup> do not seem to be affected by season or height for both fields (not shown in  
<sup>253</sup> the table). Note that, as the uncertainties in  $\beta$  and  $H$  values are significant  
<sup>254</sup> (see table 1), no definitive conclusions can be drawn on the significance of  
<sup>255</sup> highlighted tendencies. Because boundary layer is almost continuously stable  
<sup>256</sup> during winter, scaling parameters are characteristics of stable conditions dur-  
<sup>257</sup> ing this season. During summer, boundary layer is alternatively convective and

258 stable. Therefore scaling parameters are likely to be affected by both stable  
259 and convective conditions during this season.

## 260 5 Summary and Discussion

261 This study conducted an analysis of wind and temperature measurements  
262 taken at Dome C during the 2009 field campaign. First, the computation of the  
263 power spectra of wind and temperature reveals that both fields present scaling  
264 properties from 30 minutes to 10 days with a  $\beta$  exponent of approximately 2.  
265 Second, the analysis of the first-order structure function provides the degree  
266 of fractional integration in both fields (i.e.,  $H= 0.69$  for temperature and  
267  $H= 0.66$  for zonal wind). The computation of the empirical moment for the  
268 temporal gradients of the wind and temperature time series reveals multifractal  
269 behaviour. Thus, it is possible to use the universal multifractal model to fit  
270 the moment-scaling function  $K(q)$  and obtain the  $\alpha$  and  $C_1$  parameters. The  
271 same analysis is repeated for winter and summer seasons for six elevations  
272 and provides  $\beta$  and  $H$  parameters in these various conditions. While  $\beta$  and  
273  $H$  are constant with height during winter for the wind, a stratification of  $H$   
274 and  $\beta$  parameter is found during summer (e.g., from 2.06 to 2.29 for  $\beta$ ). A  
275 stratification of  $\beta$  and  $H$  parameter also exists for the temperature in both  
276 winter and summer.

277 For the first time, this analysis provides scaling parameters in Antarctica  
278 for a very stable boundary layer. An important result is the height depen-  
279 dency for  $\beta$  and  $H$  especially in summer. For the zonal wind the parameters  
280 increase from the ground to the top of the tower while for the temperature  
281 the parameters decrease from the ground to the top of the tower. This result  
282 is very surprising and to the authors best knowledge, this is the first time  
283 that such an effect has been observed in these conditions. This behaviour is

284 probably related to the different properties of turbulence at the ground and at  
285 the top of the tower due to the very strong temperature vertical gradient. In  
286 particular, a steeper slope indicates a higher correlation within data; that is  
287 turbulence could be stronger close to the ground than at higher levels. Further  
288 interpretations require additional measurements of turbulence at Dome C.

289 This analysis could be used to evaluate parametrizations used in simula-  
290 tions (Stolle et al., 2012, 2009). Indeed, many aspects of a meteorological field  
291 can be fully characterized using the multifractal approach with only few coef-  
292 ficients, e.g, the statistical moments and the probability distribution functions  
293 of the field for scales ranging from the data resolution to the time series length.  
294 Therefore, following the methodology of this paper, simulation outputs (and  
295 associated parametrizations) could be evaluated in a new and innovative way.  
296 In particular, this method could help to evaluate the statistical relationships  
297 between scales in simulations (which is not usually done to our knowledge).  
298 Moreover it will help identifying parametrizations that do not respect scaling-  
299 laws i.e., that are not physically meaningful.

300 These computed values and our conclusions must be validated with other  
301 measurements obtained in similar conditions, but to our knowledge, no previ-  
302 ous scaling (including multifractal) analysis has been conducted in the region.  
303 Finally, this analysis also highlights the intrinsic quality of our data. Indeed,  
304 most of the fitted functions were found to have relatively little noise with  
305 regard to the extreme atmospheric conditions. Since the tower still provides  
306 data, it will be possible in the future to improve the accuracy of the scaling pa-  
307 rameters. Moreover, measurements from sonic anemo-thermometers recently  
308 deployed along the tower will be highly valuable to understand the scaling  
309 properties of wind and temperature highlighted in this study.

310 **Acknowledgements** Boundary layer observation and research at Dome C were supported  
311 by the French Polar Institute (IPEV; CALVA program), Institut National des Sciences  
312 de l'Univers (Concordia and LEFE-CLAPA programs), and Observatoire des Sciences de  
313 l'Univers de Grenoble (OSUG). We are grateful to Yvon Lemaître for his precious help. The  
314 authors wish to thank two anonymous reviewers whose valuable feedback greatly improved  
315 the manuscript.

## 316 **References**

- 317 de Montera L, Barthès L, Mallet C, Golé P (2009) The effect of rain-no rain  
318 intermittency on the estimation of the universal multifractals model param-  
319 eters. *J Hydrometeor* 10:493-506, DOI 10.1175/2008JHM1040.1
- 320 Fabry F (1996) On the determination of scale ranges for precipitation fields.  
321 *J Geophys Res* 101:12,819–12,826, DOI 10.1029/96JD00718
- 322 Fraedrich K, Larnder C (1993) Scaling regimes of composite rainfall time series.  
323 *Tellus A* 45(4):289–298
- 324 Gage KS, Nastrom GD (1986) Theoretical interpretation of atmospheric  
325 wavenumber spectra of wind and temperature observed by commercial air-  
326 craft during GASP. *J Atmos Sci* 43:729–740, DOI 10.1175/1520-0469
- 327 Genthon C, Town MS, Six D, Favier V, Argentini S, Pellegrini A (2010) Mete-  
328 orological atmospheric boundary layer measurements and ECMWF analyses  
329 during summer at Dome C, Antarctica. *J Geophys Res Atmos* 115:D05104,  
330 DOI 10.1029/2009JD012741
- 331 Genthon C, Gallée H, Six D, Grigioni P, Pellegrini A (2013) Two years  
332 of atmospheric boundary layer observation on a 45-m tower at Dome C  
333 on the Antarctic plateau. *J Geophys Res Atmos* 118:3218–3232, DOI  
334 10.1002/jgrd.50128
- 335 Grachev AA, Fairall CW, Persson POG, Andreas EL, Guest PS (2005) Stable  
336 boundary-layer scaling regimes: the Sheba data. *Boundary-Layer Meteorol*

- 337 116:201–235, DOI 10.1007/s10546-004-2729-0
- 338 Hudson SR, Brandt RE (2005) A Look at the surface-based tempera-  
339 ture inversion on the antarctic plateau *J Climate* 18:1673–1696, DOI  
340 10.1175/JCLI3360.1
- 341 King JC, Turner J (1997) *Antarctic meteorology and climatology*. Cambridge  
342 University Press, Cambridge
- 343 Lavallée D, Lovejoy S, Schertzer D, Ladoy P (1993) Nonlinear variability of  
344 landscape topography: multifractal analysis and simulation. edited by L.  
345 DeCola and N. Lam In: *Fractals and Geography*, Prentice Hall, New Jersey,  
346 pp 158–192, 308 pp
- 347 Lovejoy S, Schertzer D (2010) Towards a new synthesis for atmospheric dy-  
348 namics: Space-time cascades. *Atmos Res* 96:1–52
- 349 Lovejoy S, Schertzer D (2011) Space-time cascades and the scaling of ECMWF  
350 reanalyses: Fluxes and fields. *J Geophys Res Atmos* 116:D14117, DOI  
351 10.1029/2011JD015654
- 352 Nykanen DK (2008) Linkages between orographic forcing and the scaling prop-  
353 erties of convective rainfall in mountainous regions. *J Hydrometeor* 9:327–  
354 347, DOI 10.1175/2007JHM839.1
- 355 Olsson J (1995) Limits and characteristics of the multifractal behaviour of a  
356 high-resolution rainfall time series. *Nonlinear Proc Geoph* 2:23–29
- 357 Pecknold S, Lovejoy S, Schertzer D, Hooge C, Malouin J (1993) The simu-  
358 lation of universal multifractals. edited by J. M. Perdang and A. Lejeune  
359 In: *Cellular Automata: Prospects in Astronomy and Astrophysics*, vol 1, pp  
360 228–267 World Scientific, Hackensack, N. J., 416 pp
- 361 Priestley MB (1981) *Spectral analysis and time series*. Academic Press, New  
362 York, 661 pp
- 363 Purdy JC, Harris D, Austin GL, Seed AW, Gray W (2001) A case study  
364 of orographic rainfall processes incorporating multiscaling characterization

- 365 techniques. *J Geophys Res* 106:7837–7845, DOI 10.1029/2000JD900622
- 366 Rysman JF, Verrier S, Lemaître Y, Moreau E (2013) Space-time variability of  
367 the rainfall over the western Mediterranean region: A statistical analysis. *J*  
368 *Geophys Res Atmos* 118:8448–8459, DOI 10.1002/jgrd.50656
- 369 Schertzer D, Lovejoy S (1987) Physical modeling and analysis of rain and  
370 clouds by anisotropic scaling multiplicative processes. *J Geophys Res*  
371 92:9693–9714, DOI 10.1029/JD092iD08p09693
- 372 Schmitt F, Lovejoy S, Schertzer D, Lavallée D, Hooge C (1992) Estimations  
373 directes des indices de multifractals universels dans le champ de vent et de  
374 température. *C Rendues, de l’Acad Sciences (Paris)* 314:749–754
- 375 She Z, Leveque E (1994) Universal scaling laws in fully developed turbulence.  
376 *Phys Rev Lett* 72:337–339
- 377 Stolle J, Lovejoy S, Schertzer D (2009) The stochastic multiplicative cascade  
378 structure of deterministic numerical models of the atmosphere. *Nonlinear*  
379 *Proc Geoph* 16:607–621
- 380 Stolle J, Lovejoy S, Schertzer D (2012) The temporal cascade structure of  
381 reanalyses and global circulation models. *Q J R Meteorol Soc* 138:1895–  
382 1913, DOI 10.1002/qj.1916
- 383 Tessier Y, Lovejoy S, Schertzer D (1993) Universal multifractals: theory and  
384 observations for rain and clouds *Journal of Appl Meteor* 32:223–250, DOI  
385 10.1175/1520-0450
- 386 Travouillon T, Ashley MCB, Burton MG, Storey JWV, Loewenstein RF (2003)  
387 Atmospheric turbulence at the South Pole and its implications for astron-  
388 omy. *Astron Astroph* 400:1163–1172, DOI 10.1051/0004-6361:20021814
- 389 Verrier S, Mallet C, Barthès L (2011) Multiscaling properties of rain in the  
390 time domain, taking into account rain support biases. *J Geophys Res Atmos*  
391 116:D20119, DOI 10.1029/2011JD015719

- 
- 392 Yaglom AM (1966) The influence of fluctuations in energy dissipation on the  
393 shape of turbulence characteristics in the inertial interval. Soviet Physics  
394 Doklady 11:26–30